Artigo

ISOMERIZATION-CRACKING OF N-OCTANE ON CATALYSTS BASED ON HETEROPOLYACID $H_3PW_{12}O_{40}$ AND HETEROPOLYACID SUPPORTED ON ZIRCONIA AND PROMOTED WITH Pt AND Cs

Debora L. Manuale, Gerardo C. Torres, Viviana M. Benítez, Juan M. Badano, Juan C. Yori and Jorge H. Sepúlveda*
Instituto de Investigaciones en Catálisis y Petroquímica, Facultad de Ingeniería Química – Universidad Nacional de Litoral, Consejo Nacional de Investigaciones Científicas y Técnicas, Santiago del Estero 2654, 3000 - Santa Fe, Argentina

Recebido em 10/9/12; aceito em 1/3/13; publicado na web em 4/6/13

Isomerization–cracking of n-octane was studied using $H_3PW_{12}O_{40}$ (HPA) and HPA supported on zirconia and promoted with Pt and Cs. The addition of Pt and Cs to the supported HPA did not modify the Keggin structure. The Pt addition to the supported HPA did not substantially modify the total acidity; however, the Brönsted acidity increased significantly. Cs increased the total acidity and Brönsted acidity. A linear relation was observed between the n-C_8 total conversion and Brönsted acidity. The most adequate catalysts for performing isomerization and cracking to yield high research octane number (RON) are those with higher values of Brönsted acidity.

Keywords: reformulated fuels; supported heteropolyacids.

INTRODUCTION

The worldwide trend for the replacement of low-octane gasolines with premium gasolines and the increased use of diesel fuels has increased in recent years. The choice of diesel fuels is supported by the higher thermodynamic efficiency of the diesel motor. This trend produces an imbalance and generates refinery stocks that are difficult to use, thus making refiners seek technical solutions for increasing the ratios of diesel/gasoline and of premium/standard gasoline. Another important issue is the need to upgrade heavy cuts and other low-cost feedstocks to increase the throughput of gasoline and diesel pools, thus improving the profitability of the refinery. In the case of gasoline, one attractive option is to process waxy feedstocks[1-4], which demands the use of the hydroisomerization–cracking process to form branched paraffins with high octane numbers. Alkanes with more than seven carbon atoms are easily cracked; thus, the requirements for long paraffin isomerization–cracking catalysts are as follows: (i) high selectivity for branched isomers; (ii) low selectivity for light gases; and (iii) low environmental impact.

Therefore, the first catalytic issue is the correct distribution of acid strengths of these catalysts. Acidity requirements increase in inverse proportion to the length of the chain, with the general understanding that the longer the chain the higher the reactivity of the paraffin. Cracking is always more demanding than skeletal branching. This is one reason why cracking can sometimes proceed after skeletal branching has occurred on the same acid site. The consequences of an inappropriate acid strength distribution are easily foreseen. If the acid sites are too strong, extensive cracking occurs with the combined disadvantages of low liquid yield and premature catalyst coke fouling. On the other hand, if the acid sites are too weak, isomerization might occur, but cracking will be highly disfavored. Hence, inconveniently long isomers of low volatility and low octane number are obtained.[5]

Some isomerization catalysts currently in use are corrosive and contaminating (sulfuric acid, fluorhydric acid, alumina-supported $AlCl_3$, etc), and their disposal poses many problems to refiners. High liquid yields and high selectivity for branched isoparaffins can be notably obtained by using oxoanion-promoted zirconia catalysts. These catalysts, tungsten–zirconia (WO_3–ZrO_2) and sulfate–zirconia (SO_4^{2-}–ZrO_2), have outstanding properties of high activity and selectivity at low temperatures. A great amount of literature has been published in recent years on the preparation and characterization of such catalysts.[6-10] Pt/WO_3–ZrO_2 (Pt/WZ) is the commercial catalyst of the C_5–C_6 virgin naphtha isomerization process, EMICT (Exxon-Mobil Isomerization Catalyst). Moreover, this catalyst has been successfully tested for isomerization–cracking reactions of heavy paraffin for producing isomerizates of a high octane number for adding to the gasoline pool. One of the drawbacks for this application is the low resistance of the catalyst to many poisons (water < 10–20 ppm, sulfur < 0.1 ppm, aromatics < 5%).[11,12] Therefore, all efforts to overcome these drawbacks are welcome. Another possibility is to develop new isomerization–cracking catalysts with improved performance.

In a previous study, we studied the hydroisomerization–cracking reaction of n-octane using heteropolyacids (HPA), grafted on several supports (zirconia, silica, and carbon) and promoted with Pt.[13] Supported HPA samples showed higher specific activity values for HPA than pure HPA. The Pt addition had two effects: it increased the activity for n-octane (n-C_8) hydroconversion and the stability of the catalysts. Similar results were obtained by Yang et al. who studied the catalytic properties of Pt-promoted-heteropoly-compound/Al-MCM-41 hybrid catalysts.[14]

In this study, we investigated whether different HPA-based catalysts could be an alternative catalyst to Pt/WZ for the isomerization–cracking reaction of heavy paraffins. The main objectives were as follows: (i) comparing the catalytic performance of different HPA-based catalysts (with known Pt/WZ catalysts for the isomerization–cracking of n-C_8 used as model molecule) to elucidate the properties that have a meaningful impact on the catalyst activity and reaction mechanism; (ii) defining some aspects of the Pt-HPA/Z preparation technique that have not been studied before, e.g., the most convenient method for incorporating Pt and HPA on the support.

EXPERIMENTAL

Catalyst preparation

Zirconium hydroxide (ZH) was obtained by the hydrolysis of zirconium oxychloride ($ZrOCl_2.8H_2O$, Strem Chemicals, 99.998%) followed by precipitation with an ammonia solution. The precipitate

*e-mail: jsepulve@fiq.unl.edu.ar

was washed and dried in a stove at 110 °C overnight. ZrO_2 (Z, 59 m^2/g) was obtained by the calcination of ZH in air for 3 h at 620 °C. Tungstophosphoric acid, $H_3PW_{12}O_{40}.6H_2O$ (HPA), was supplied by Merck.

HPA was supported on Z by incipient wetness impregnation. The volume and concentration of the solutions were adjusted to get a concentration of 30% HPA in the final catalyst. After impregnation, the catalyst was dried in a stove for 12 h at 110 °C and then calcined in air for 3 h at 500 °C. The HPA content was assessed by atomic absorption spectroscopy.Pt-HPA was prepared by mixing HPA and chloroplatinic acid solutions (H_2PtCl_6, Merck >99.5%) in adequate concentrations to get 1% Pt in the final catalyst. The final solid was filtered and then dried in a stove for 12 h at 100 °C. Then, the solid was treated in air at 500 °C for 3 h to eliminate chlorine from the catalyst.

Cs-HPA was prepared from aqueous HPA and Cs_2CO_3 solutions (Sigma, >99.0%) as reported elsewhere.[15] The Cs_2CO_3 solution was added dropwise to an HPA solution at room temperature. The concentrations of both solutions were adjusted to get a precipitate with the nominal composition of $Cs_{2.5}H_{0.5}PW_{12}O_{40}$. The final solid was filtered and then dried in a stove for 12 h at 100 °C and finally calcined at 300 °C for 3 h.

Pt-HPA/Z (A) was prepared by the incipient wetness impregnation of HPA/Z with an aqueous H_2PtCl_6 solution in an adequate concentration to get 1% Pt in the final catalyst. The sample was dried at 110 °C in air overnight and then treated in air at 500 °C for 3 h to eliminate chlorine from the catalyst.

Pt-HPA/Z (B) was prepared by the incipient wetness co-impregnation of the zirconia support (Z) with aqueous HPA and H_2PtCl_6 solutions. The amount of each solution was regulated to get about 30% and 1% Pt in the final catalyst. Then, the catalyst was treated in the same way as Pt-HPA/Z (A).

WOx-ZrO_2 (WZ) was obtained by the impregnation of ZH with an ammonium metatungstate solution, which had been previously stabilized at pH 6. This procedure is known to enrich the solution with medium-sized tungstate anions. The volume and concentration of the solution were adjusted to get 15% W in the final catalyst.[16] Pt/WZ was obtained by incorporating Pt into the WZ supports by impregnation to incipient wetness with a H_2PtCl_6 solution. The volume and concentration were adjusted to obtain 1% Pt in the final catalyst. Then, the catalyst was dried at 110 °C and calcined in air for 3 h at 500 °C.

Prior to the test reactions, the catalysts were subjected to a pretreatment of reduction at 300 °C in H_2 for 1 h for completely reducing the catalyst to metallic Pt.[17]

Catalyst characterization

XRD measurements were performed using a Shimadzu DX-1 diffractometer with Cu-Kα radiation filtered with Ni. Spectra were recorded in the 20° to 65° 2θ range, and the scanning rate was 1.2° min^{-1}. For Pt/WZ, the peaks located at 28° and 31° were attributed to the monoclinic phase of zirconia and those located at 30° to the tetragonal phase. The peaks located in the 23–25° range were attributed to WO_3 crystals.

The supported HPA samples were also characterized by FTIR absorption spectroscopy. The FTIR spectra of degassed supported HPA samples were taken at room temperature on a Shimadzu FT-IR-8101 spectrophotometer over the 4800–400 cm^{-1} range and with a resolution of 4 cm^{-1}. Self-supported wafers were outgassed at 10^{-6} Torr at 100 °C for 1 h before recording each spectrum.

The specific surface areas of the catalysts were measured using the isotherm of adsorption of nitrogen at 77 K using Micromeritics 2100 E equipment. The samples were degassed at 200 °C for 2 h under vacuum.

The amount of acid and acid strength were assessed by the temperature-programmed desorption of probe molecules. 2,4,6-Trimethylpyridine (TMP, collidine, Merck, synthesis reagent, > 98% by GC assay) was used as a probe for Brönsted acid sites, and pyridine (Py, Merck, >98%) was used to test Brönsted and Lewis acid sites.[18] The samples were first immersed in an excess volume of the pure reactants at room temperature for 6 h. Then, they were filtered and dried in air in an open vial at room temperature. The samples were placed in a quartz microreactor and stabilized in N_2 for 1 h at 100 °C. Then, they were heated from 100 °C to 650 °C at 10 °C min^{-1}. The desorbed products were continuously analyzed with an FID detector.

Catalytic tests

Hydroisomerization–cracking of n-octane: A catalyst weighing 0.25 g was used in each test reaction, which was crushed and sieved to 35–80 meshes. A tubular quartz reactor (½" I.D. and length of 2") was used, and reaction conditions were 0.1 MPa, 300 °C, WHSV = 4 h^{-1}, and molar ratio $H_2/n\text{-}C_8 = 6$. The products were analyzed on-line using chromatography with a 100-m capillary column coated with squalene and an FID detector. Catalytic evaluations were carried out in duplicate within an experimental error of less than 5%. The range of products was determined by their retention time after calibration with known standards. From chromatographic data, the conversion to and selectivity for different reaction products were calculated (on a carbon basis).

The selectivity for each product i was defined as follows: *Ai* is the area of the chromatographic peak of product *i*, *fi* is its response factor, *ni* is the number of carbon atoms of *i*, and *Mi* is its molecular weight.

$$Si(\%) = \frac{(yeld\ of\ i)(\%)}{X(\%)} \times 100 = \frac{Ai \times fi \times ni}{Mi\left(\sum \frac{Ai \times fi \times ni}{Mi}\right)X} \times 100$$

The research octane number (RON) was calculated using a non-linear method, which used the GC compositional data and the measured pure and blending RON values of various hydrocarbons, which are widely published.[19] This method, which utilizes calculable weighting factors specific for each gasoline blend, showed excellent agreement with the RON values measured in a standard CFR engine. The RON gain was calculated as the difference between the RON of the mixture and that of n-octane.

The amount and nature of the coke deposited on the catalysts at the end of the tests was determined by temperature-programmed oxidation (TPO). The coked catalyst (0.04–0.06 g) was loaded in a quartz reactor and stabilized in N_2. Then, the nitrogen stream was replaced by a mixture of 5% O_2 in N_2 (60 cm^3 min^{-1}), and the cell temperature was increased from 30 °C to 650 °C at a heating rate of 10 °C min^{-1}. Coke deposits were burned, and the combustion gases that were converted to methane were quantitatively continuously measured by an FID detector. The total carbon concentration of the catalyst samples was obtained by the integration of the TPO trace and TPO tests of samples with a known amount of carbon used as reference.[20]

RESULTS AND DISCUSSION

Catalyst characterization

XRD spectra of HPA, Cs-HPA, and Pt-HPA are shown in Figure 1. The obtained spectra were similar. Differences in the peak intensity were due to the various degrees of hydration of samples after calcination in air (Cs-HPA at 300 °C, HPA and Pt-HPA at 500 °C). HPA and Pt-HPA have a lower degree of hydration, and they appear

almost amorphous by XRD. It can then be concluded that the addition of Pt or Cs does not modify the basic Keggin structure of HPA. Moreover, in both cases, the diffractograms did not present peaks of Pt or Cs as separate phases, suggesting that both metals were incorporated into the Keggin structure of HPA. However, in the case of Pt-supported catalysts, the final Pt content is relatively low for identification by XRD.

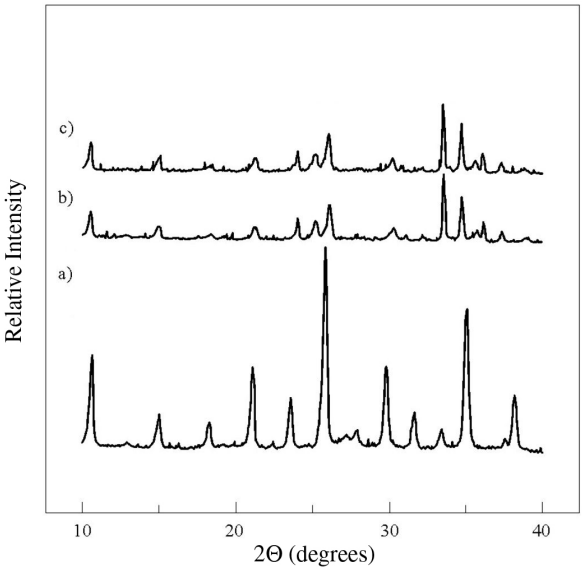

Figure 1. *XRD spectra. a) Cs-HPA, b) HPA, c) Pt-HPA*

The XRD spectra of Pt/WZ revealed that the tetragonal structure of zirconia is stabilized after calcination at 700 °C.[16] No peaks attributable to the monoclinic phase of zirconia (e.g., 28° and 31°) were detected. The peaks observed at 23° to 25° were attributed to WO_3 crystals.

The supported HPA species were identified by FTIR spectroscopy. The Keggin structure of HPA has four absorption bands at characteristic wavelengths in the 800–1110 cm^{-1} range. These bands can be attributed to the different absorption modes of the $[PW_{12}O_{40}]^{3-}$ primary structure.[21,22] The peaks located at 1080 cm^{-1}, 985 cm^{-1}, 893 cm^{-1}, and 812 cm^{-1} corresponded to the four stretching vibration modes of the oxygen atoms bound to W and P, which are identified as ν (P–O), ν (W=O), ν $(W–O–W)_{edge}$, and ν $(W–O–W)_{corner}$, respectively.

Table 1 shows compositions and specific surface area (Sg) values of the prepared samples. After calcination in air at 500 °C, HPA had a low specific surface area. When supported over Z, the specific surface area of the new material was the same as that of the single support (Z) calcined at the same temperature (59 $m^2\ g^{-1}$). The same happens with Pt-HPA/Z, (A) and (B). The incorporation of Pt into HPA/Z did not modify the specific surface area of the latter. Pt/WZ had a specific surface area of 60 $m^2\ g^{-1}$.

HPA salts have been reported to maintain their Keggin structure by the addition of different metallic ions.[23,24] Niiyama et al.[24] made the following classification: (i) small metal ions like Na^+ and Cu^{2+}, and (ii) a second group of large metal ions such as Cs^+ and Pd^{2+}. The group (i) salts usually possess low surface area, high solubility in water, and the capability to absorb polar or basic molecules from the solid bulk. In contrast, group (ii) salts usually have high specific surface areas, insoluble in water, and are unable to absorb molecules. Species such as $Pd_{1.5}H_{1.5}PW_{12}O_{40}$, $Cs_{2.5}H_{0.5}PW_{12}O_{40}$, and $Ag_3PW_{12}O_{40}$ have been reported, and Pt belongs to this group.

When HPA and chloroplatinic acid solutions were mixed, an insoluble precipitate was formed, which was probably $Pt_xH_{3-x}PW_{12}O_{40}$. After drying and calcination at 500 °C, the specific surface area of this compound is two times that of HPA. When solutions of HPA and a Cs salt were mixed, an insoluble precipitate was formed, which had a specific surface area of 140 m^2g^{-1} after being dried and calcined at 300 °C. This value is typical of $Cs_{2.5}H_{0.5}PW_{12}O_{40}$.[25] The differences in the increase in surface area produced by the addition of Pt and Cs addition are quite marked. Pt only duplicates the surface area value of HPA, but Cs increases it by 24 times. The reasons for this difference could be a priori related to the following: i) the different contents of Pt and Cs added (1.0 and 10.35 wt %, respectively) and ii) the different calcination temperature of each catalyst. It is convenient to recall that both solids, Cs-HPA and Pt-HPA, have the same Keggin structure as HPA. The previous remarks validate the hypotheses that Cs and Pt are incorporated into the Keggin structure of HPA, forming a new species.

Table 1 also shows a quantitative comparison of the total acidity (total amount of desorbed pyridine expressed as μmol per gram of HPA) and Brönsted acidity (total amount of TMP desorbed expressed as μmol per gram of HPA). HPA has the lowest total acidity. After treatment at 500 °C, a significant amount of water was lost. Hence, the Brönsted acidity of HPA was low. When HPA was promoted with Pt, the total acidity was not modified, but the Brönsted acidity increased. The addition of Cs produced an increase in the total acidity and Brönsted acidity. In the case of supported samples, the total and Brönsted acidities increased 3-fold. It can be concluded that the addition of Pt or Cs to HPA modifies many of its properties (specific surface area, total acidity, and Brönsted acidity) but does not modify the Keggin structure.

The addition of Pt to the supported HPA samples did not modify the total acidity substantially, but the Brönsted acidity increased remarkably. The Pt/WZ shows total and Brönsted acidity values similar to those of the Pt-promoted HPA/Z catalysts. This is very important; earlier, we marked the importance of catalyst acidity to obtain high liquid yields of and high selectivity for branched isoparaffins. The total acidity rank is as follows: Pt-HPA/Z (A) > Pt-HPA/Z (B) > HPA/Z > Pt/WZ > Cs-HPA > Pt-HPA~HPA. On the other hand, the order with respect to Brönsted acidity is as follows: Pt-HPA/Z(A) > Pt-HPA/Z (B) > Pt/WZ > Pt-HPA~ Cs-HPA~HPA/Z > HPA.

Figure 2 shows the conversion of n-octane as a function of the reaction time. All catalysts show similar trends with increasing time-on--stream (TOS). Deactivation was a consequence of the formation of

Table 1. Catalyst properties

Catalysts	HPA (%)	Pt, Cs (%)	Sg ($m^{2\times}g^{-1}$)	Total acidity [μmol Py g^{-1}]	Brönsted acidity [μmol TMP g^{-1}]
HPA	100	--	5	40.3	1.5
HPA/Z	29	--	58	127.6	8.98
Pt-HPA	99.1	0.9	13	42.0	10.0
Cs-HPA	89.65	10.36	140	98.0	7.55
Pt-HPA/Z (A)	29	0.9	57	134.2	75
Pt-HPA/Z (B)	28.7	1.0	55	130.1	69
Pt/WZ	--	1.0	60	104	64

surface coke being faster during the first 20 min. All samples showed higher activity values than HPA. When considering the conversion values at 5 min, the order of the activity is as follows: Pt-HPA/Z(B) ~ Pt-HPA/Z(A) > Pt/WZ >> Cs-HPA ~ Pt-HPA > HPA/Z > HPA.

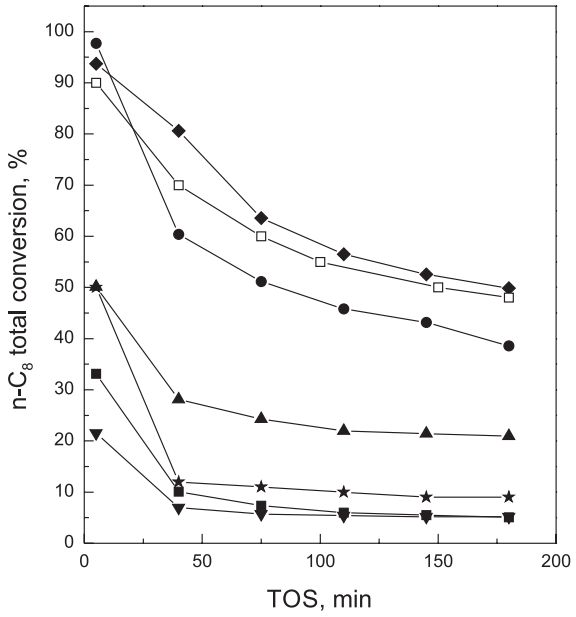

Figure 2. *Hydroconversion of n-C_8 as a function of time on stream of the catalysts. ●: Pt-HPA/Z (B), ■: HPA/Z, ▲: Pt-HPA, ◆: Pt-HPA/Z (A), ★: Cs-HPA, ▼: HPA, □: Pt/WZ*

An analysis of the catalytic activity and the structural properties of the catalysts is necessary to elucidate the properties that have a meaningful impact. *A priori* no correlation could be obtained between the activity of the catalysts and the HPA content, specific surface area, or total acidity. However, for all samples, the activity order practically coincided with the Brönsted acidity rank. A linear relation between the n-C_8 total conversion at 5 min of TOS and the Brönsted acidity of the catalysts can be seen in Figure 3.

The addition of Cs to HPA produced a significant increase in the total acidity, much greater than that produced by Pt. However, in both cases, the values of Brönsted acidity are similar, and therefore, both catalysts have similar values of conversion at 5 min of TOS.

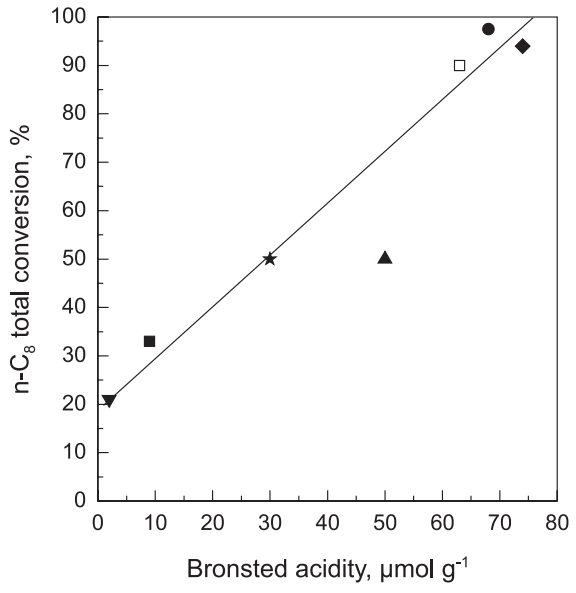

Figure 3. *Hydroconversion of n-C_8 as a function of Brönsted acidity of catalysts. ●: Pt-HPA/Z (B), ■: HPA/Z, ▲: Pt-HPA, ◆: Pt-HPA/Z (A), ★: Cs-HPA, ▼: HPA, □: Pt/WZ*

Pt-HPA is stabilized after 1 h of reaction with a higher conversion value than Cs-HPA. Therefore, it could be concluded that the addition of Pt to HPA is more beneficial than the addition of Cs for this type of reaction. In this sense, a small percentage of Pt is known to generate sufficient activated hydrogen to hydrogenate coke precursors and stabilize the catalyst during reaction.

In the case of the supported samples, the effect of Pt is more marked, the total conversion being increased 3-fold. Both samples, Pt-HPA/Z(A) and Pt-HPA/Z(B), have similar values of Brönsted acidity and initial conversion. However, the samples had different deactivation rates, where that of Pt-HPA/Z(B) is higher than that of Pt-HPA/Z(A). Pt-HPA/Z(A) and Pt/WZ show similar patterns of conversion as a function of time (deactivation rates). After 175 min of TOS, the conversion level is the highest for Pt-HPA/Z(A), followed by Pt/WZ and Pt-HPA/Z(B). Pt-HPA/Z(A) and Pt/WZ had a higher resistance to the formation of coke (47% activity loss), while in the case of Pt-HPA/Z(B), the resistance is lower (59% activity loss). This is an important difference, and therefore, it can be concluded that the sequence and method of addition of Pt and HPA to Z affect the stability of the obtained catalysts. On the other hand, we can say that Pt-HPA/Z(A) is an interesting alternative catalyst to Pt/WZ.

TOF values (expressed as nC_8 molecules converted per surface active site per time) of the prepared catalysts are presented in Table 2. These values were calculated from the initial conversion as a function of the total acidity and Brönsted acidity. TOF values are useful for predicting possible changes in the nature of the active sites, in this case due to Zr (in the supported catalysts) and Pt and Cs incorporation into HPA. The obtained TOF values indicate that the nature of the active sites of HPA was changed. Considering Brönsted acid active sites, we could conclude that the introduction of other atoms into the HPA structure diminishes the intrinsic activity of the active site. Similar results were previously reported by Ivanov et al.[23] However, this effect is largely compensated by the generation of a greater amount of proton active sites.

Table 2. TOF values of the catalysts

Catalysts	TOF^{TA} [s^{-1}]	TOF^{BA} [s^{-1}]
HPA	1.6	43.1
HPA/Z	0.8	11.7
Pt-HPA	3.7	15.4
Cs-HPA	1.6	20.4
Pt-HPA/Z (A)	2.2	3.9
Pt-HPA/Z (B)	2.3	4.4
Pt/WZ	2.7	4.3

TOF^{TA} : expressed as nC_8 molecules converted per total acid active site per second. TOF^{TA} : expressed as nC_8 molecules converted per Brönsted acid active site per second.

The temperature-programmed oxidation of the coke deposits was performed on samples that presented higher activity levels after 175 min of TOS (Table 3). The integration of the area under the TPO trace yields the total amount of deposited carbon. The coke content of these catalysts was small (<1%), indicating that only a small fraction of the surface sites was affected by it. These carbon deposits would be too small to explain the decrease of the conversion in the tested samples.

In all cases, the TPO traces showed a big peak at 350 °C–500 °C, corresponding to the combustion of highly polymerized, hydrogen--deficient coke located on the acid sites of the support. No peaks at

Table 3. Coke deposition on catalysts after 175 min TOS

Catalysts	Carbon (%)
Pt/HPA-Z (A)	0.4
Pt/HPA-Z (B)	0.7
Pt/WZ	0.8

200 °C–350 °C, attributable to the combustion of poorly polymerized hydrogen-rich coke, typically located on the metal particles or their surroundings, were seen.[26] One possible explanation for coking behavior is that it is influenced by mass-transfer limitations appearing after the blocking of the catalyst pores. However, this is not possible because of the small volume of carbon produced and the relatively big diameter of the catalyst pores. Another more likely explanation is that the catalytic activity and stability are related to the relative concentration of Lewis and Brönsted acid sites.

Table 4 shows the selectivity values for normal paraffins and isoparaffins and for major reaction products with respect to different catalysts at 5 min of TOS (results corresponding to the fresh, coke-free catalysts). All catalysts show a similar pattern of product distribution. It is observed that

(i) Most products are normal paraffins and isoparaffins.

(ii) Cyclization reactions occur with lower than 3% yield.

(iii) The iso/normal paraffin ratio is greater than 1 in all series.

(iv) i-C_4, i-C_5, and i-C_8 dominate the isoparaffin distributions, while i-C_6 and i-C_7 are negligible.

(v) The relation i-C_4/n-C_4 is above the thermodynamic equilibrium value for the isomerization reaction varying between 2.2 and 3.7.[27]

(vi) The fraction of the C_8 isomers is mainly composed of monobranched isomers (2-methyl heptane and 3-methyl heptane) in a 5:1 ratio with respect to the multibranched isomers. The order is mono >> di >> tribranched isomer.

(vii) Compounds with more than eight carbon atoms were not detected.

A greater concentration of isoparaffins is expected from thermodynamics. The well-accepted classical mechanism of isomerization and cracking of a linear paraffin necessarily begins with the adsorption of a carbenium ion. This is possibly isomerized initially in the adsorbed state by any of the accepted mechanisms, such as a methyl shift or the formation of protonated cyclopropanes. Cracking is a consecutive reaction. The branched isomer (mono, di, or tri) can be cracked on the same site or can readsorb on another site and be cracked there. Cracking can only proceed on strong acid sites. In an ''ideal'' isomerization–cracking scheme, molecules that result from primary cracking are desorbed and are not subjected to secondary cracking, and in this manner, the formation of light gaseous products is minimal.[28-30] Considering that the isomerization step of n-C_8 mainly produces monobranched isomers, the same can be cracked to yield the following pairs: i-C_4 + n-C_4, i-C_5 + C_3, i-C_6 + C_2. The last pair is the least feasible, and the first two pairs are more likely to be cracked, because long molecules tend to be broken in the middle positions. The first pair corresponds to the cracking of 2-methyl heptanes, and the second pair corresponds to the cracking of 3-methyl heptane.

As can be seen in Table 4, in all cases, i-C_4 is the most abundant isomer, confirming that cracking is favored in the middle position of a long paraffin molecule. i-C_5 is produced to a lesser extent than i-C_4. The relationship of the rupture of the pairs (i-C_4 + n-C_4) / (i-C_5 + n-C_3) is about 3/1.

The molar ratio of i-C_5/C_3 in all cases is approximately 1. On the other hand, a value greater than unity for the i-C_4/n-C_4 and C_3/n-C_5 molar ratio rule out other mechanisms such as the direct cracking of n-C_8 into two n-C_4 or C_3 + n-C_5 pairs. Moreover, this would indicate that i-C_4 does not originate only from the cracking of monobranched i-C_8. Two other routes are as follows: i) the isomerization of n-C_4, a product of the cracking of i-C_8 and the cracking of di-branched i-C_8 and ii) the further isomerization of the n-C_4 product of the cracking reaction of i-C_8. Of the two possibilities, the last is the most feasible, because in hydrocracking reactions, branched products cannot be formed by the secondary isomerization of the linear fragments, since competitive adsorption at the acid sites becomes less favorable with the decreasing chain length of a fragment.[4,31] On the other hand, it is well-known that cracking reactions are slower than isomerization; thus, the formation of cracking products must follow the formation of branched isomers. Rezgui et al. reported that for the hydroconversion of n-C_8, the ratio of mono- to multibranched isomers increased with space velocity, which infers that isomerization first predominantly leads to monobranched isomers and then to multibranched ones. Multibranched isomers are more easily cracked than monobranched ones.[4]

Depending on the amount of acid sites and the residence time, the molecule can consecutively react on more than one site. In this manner, cracked paraffins can be reacted again. If one acid site is sufficiently strong to retain the molecule after cracking, consecutive reactions may occur on the same site. The low amount of C_2 obtained in all cases indicates that no secondary cracking occurs. The absence of compounds with more than eight carbon atoms rules out the possibility of the dimerization of the n-C_8 pathway.

The absence of C_1 and the low yield of aromatization products are related to the inhibition of the metal function of Pt-containing catalysts. In the case of Pt/WZ catalysts, there exists a strong interaction between the support and the metal Pt particles, which is seemingly related to the decoration of Pt particles with WO_x species during heat treatments. The electronic density of Pt is depleted, and $Pt^{\delta+}$ domains are generated, which coexist with Pt^0 on the surface.[7] This phenomenon weakens the activity of the metal function. In the case of the Pt-doped HPA catalysts, a similar phenomenon could be happening.

Finally, according to the obtained results, we can conclude that on the studied catalysts, the mechanism of n-octane conversion can be described by the simple scheme shown in Figure 4: n-C_8 is first isomerized over an acid site to give monobranched i-C_8. One part of the produced monobranched i-C_8 could be isomerized again over the same or other acid site. Then, dibranched i-C_8 is cracked to mainly

Table 4. Hydroconversion of n-octane; selectivities of the catalysts at 5 minutes on stream

Catalyst	S_{nP} (%)	S_{iP} (%)	Selectivity for products (%)					
			C_3	iC_4	nC_4	iC_5	nC_5	iC_8
HPA	31.6	65.9	14.4	39.1	13.8	16.3	3.4	10.4
HPA/Z	29.6	68.4	14.0	46.6	12.7	17.3	2.9	4.6
Pt-HPA	34.9	63.9	14.4	35.4	16.1	17.0	4.4	11.5
Cs-HPA	35.0	62.8	13.9	34.0	15.8	16.8	3.9	12.0
Pt-HPA/Z(A)	35.5	61.9	11.9	38.5	18.0	13.3	5.6	10.1
Pt-HPA/Z(B)	34.5	62.9	10.8	39.1	17.0	14.8	6.0	9.0
Pt/WZ	35.0	63.3	10.3	35.9	15.9	11.8	4.9	15.6

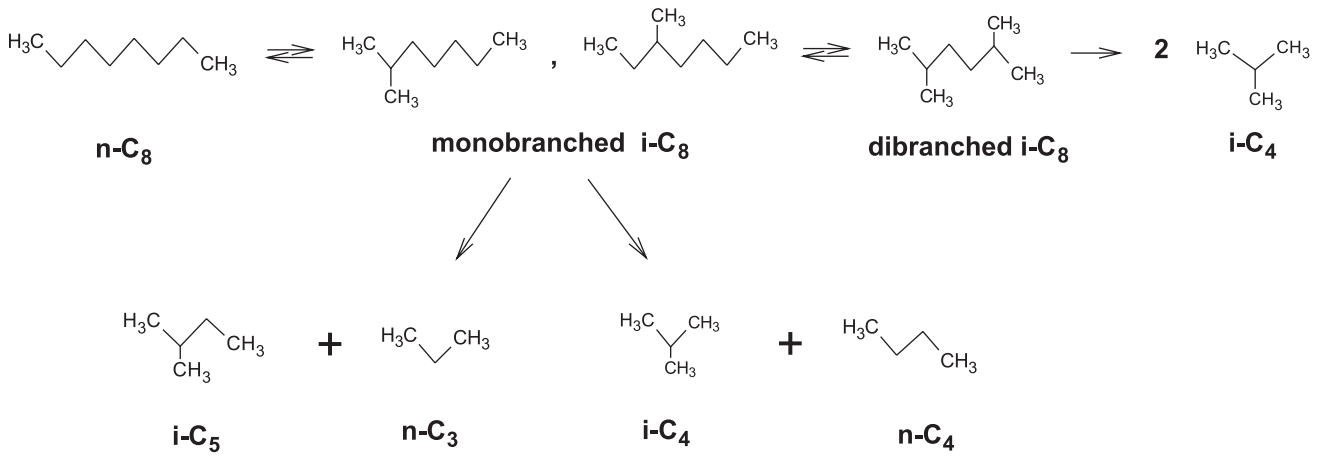

Figure 4. *Hydroconversion of n-C_8 reaction pathway*

yield i-C_4. The other part of monobranched isomer is cracked to yield one of the (i-C_4 + n-C_4) or (i-C_5 + C_3) pairs.

Figure 5 shows a plot of the RON gain as a function of the Brönsted acidity. The RON of the mixture was calculated with the yield values at 5 min of TOS. A linear correlation exists between the two quantities. The catalysts produce 17–114 additional RON points. Cs-HPA and Pt-HPA produce only moderate RON gains, while Pt/WZ produces 86 additional points. Pt-HPA/Z(B) yields a RON gain of 114 points and Pt-HPA/Z(A) 104 points. The explanation is simple: higher values of Brönsted acidity produce higher yields of i-C_4 and i-C_5, compounds that yield 130 and 100 points of blending RON, respectively. Mono- and dibranched C_8 isomers supply only 30 points to the hydrocarbon mixture. Compared to Pt/WZ, Pt-HPA/Z(A) catalysts seem more adequate for undertaking the isomerization–cracking of heavy paraffinic feedstocks.

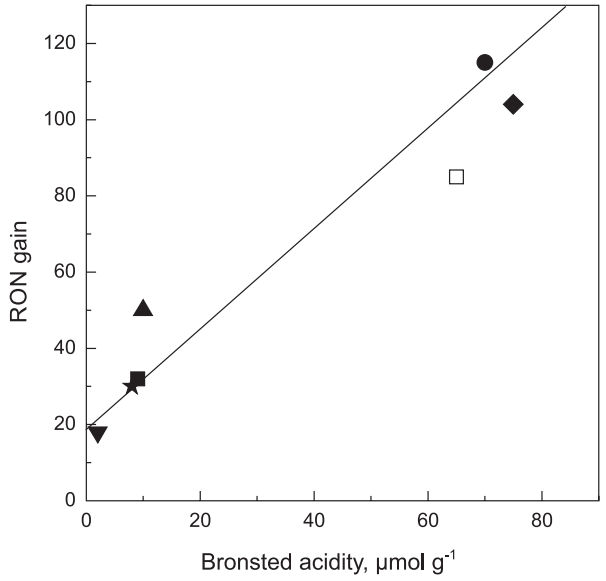

Figure 5. *RON gain as a function of Brönsted acidity of catalysts. ●: Pt-HPA/Z (B), ■: HPA/Z, ▲: Pt-HPA, ◆: Pt-HPA/Z (A), ★: Cs-HPA, ▼: HPA, □: Pt/WZ*

CONCLUSIONS

The addition of Pt or Cs to HPA-supported catalysts did not produce changes in the Keggin structure. The initial activity of isomerization–cracking of n-octane showed a linear correlation with the Brönsted acidity of the catalysts. Also, the manner of incorporating Pt and HPA into the support was important for the stability of catalyst, which perhaps can be related to the presence of $Pt_x H_{3-x}PW_{12}O_{40}$.

All catalysts showed a similar pattern of product selectivity. The results pointed to a simple transformation mechanism, in which n-C_8 is isomerized first over an acid site to give monobranched i-C_8. One part of the produced monobranched i-C_8 could be isomerized again over the same or other acid site. Then, dibranched i-C_8 is cracked to mainly yield i-C_4. The other part of monobranched isomers is cracked to yield one of the (i-C_4 + n-C_4) or (i-C_5 + C_3) pairs. Therefore, the RON upgrade of the isomerizate and conversion are proportional to the Brönsted acidity.

ACKNOWLEDGEMENTS

This work was supported with funding of Consejo Nacional de Investigaciones Científicas y Tecnológicas (CONICET) and Universidad Nacional del Litoral (UNL) of Argentina.

REFERENCES

1. Weitkamp, J.; *Ind. Eng. Chem. Prod. Res. Dev.* **1982**, *21*, 550.
2. Calemma, V.; Petrello, S.; Perego, C.; *Appl. Catal. A* **2000**, *190*, 207.
3. Weihe, M.; Hunger, M.; Breuninger, M.; Karge, H. G.; Weitkamp, J.; *J. Catal.* **2001**, *198*, 256.
4. Rezgui, Y.; Guemini, M.; *Energy Fuels* **2007**, *21*, 602.
5. Busto, M.; Vera, C. R.; Grau, J. M.; *Fuel Process. Technol.* **2011**, *92*, 1675.
6 Martínez, A.; Prieto, G.; Arribas, M. A.; Concepción, P.; Sánchez-Royo, J. F.; *J. Catal.* **2007**, *248*, 288.
7 Vu, T. N.; van Gestel, J.; Wilson, J. P.; Collet, C.; Dath, J. P.; Duchet, J. C.; *J. Catal.* **2005**, *231*, 468.
8 Busto M.; Benítez, V. M.; Vera, C. R.; Grau, J. M.; Yori, J. C.; *Applied Catal. A: General* **2008**, *347*, 117.
9 Zhou, Z.; Zhang, Y.; Tierney, J. W.; Wender, I.; *Fuel Process. Technol.* **2003**, *83*, 67.
10 Benítez, V. M.; Yori, J. C.; Vera, C. R.; Pieck, C. L.; Grau, J. M.; Parera, J. M.; *Ind. Eng. Chem. Res.* **2005**, *44*, 1716.
11 Beck, J., "EMICT, A Regenerable Paraffin Isomerization Catalyst", MCCJ 15th Anniversary Symposium, **2000**.
12 Busto, M.; Grau, J. M.; Canavese, S.; Vera, C. R.; *Energy Fuels* **2009**, *23*, 599.
13 Yori, J. C.; Grau, J. M.; Benítez, V. M.; Sepúlveda, J.; *Appl. Catal. A* **2005**, *286*, 71.
14 Yang, X. K.; Chen, L. F.; Wang, J. A.; Noren, L. E.; Novaro, A.; *Catal. Today* **2009**, *48*, 160.

15. Sepúlveda, J. H.; Vera, C. R.; Yori, J. C.; Badano, J. M.; *Quim. Nova* **2011**, *34*, 601
16. Busto, M.; Benítez, V. M.; Vera, C. R.; Grau, J. M.; Yori, J. C.; *Appl. Catal. A* **2008**, *347*, 117.
17. Grau, J. M.; Vera, C. R.; Benitez, V. M.; Yori, J. C.; *Energy Fuels* **2008**, *22*, 1680
18. Vicerich, M. A.; Especel, C.; Benitez, V. M.; Epron, F.; Pieck, C. L.; *Appl. Catal. A* **2011**, *407*, 49.
19. Nikolaou, N.; Papadopoulos, C. E.; Gaglias, I. A.; Pitarakis, K. G.; *Fuel* **2004**, *83*, 517.
20. Carvalho, L. S.; Conceicão, K. C. S.; Mazzieri, V. A.; Reyes, P.; Pieck, C. L.; do Carmo Rangel, M.; *Applied Catalysis A: General* **2012**, *156*, 419.
21. Kovalchuk, T. V.; Kochkin, Ju, N.; Sfihi, H.; Zaitsev, V. N.; Fraissard, J.; *J. Catal.* **2009**, *263*, 247.
22. Kim, J. K.; Choi, J. H.; Song, J. H.; Yi, J.; Song, I. K.; *Catal. Commun.* **2012**, *27*, 5.
23. Ivanov, A. V.; Vasina, T. V.; Nissenbaum, V. D.; Kustov, L. M.; Timofeeva, M. N.; Houzvicka, J. I.; *Appl. Catal. A* **2004**, *259*, 65.
24. Niiyama, H.; Saito, Y.; Echigoya, E.; *Proceedings of the Seventh International Congress on Catalysis*, Tokyo, Elsevier: Amsterdam, 1980, p. 1416.
25. Balbinot L.; Schuchardt U.; Vera C.; Sepúlveda J.; *Catal. Commun.* **2008**, *9*, 1878
26. Pompeo, F.; Resasco, D. E.; *Nano Lett.* **2002**, *2*, 369
27. Parera, J. M.; *Catal. Today* **1992**, *15*, 481.
28. Martens, J. A.; Vanbutsele, G.; Jacobs, P. A.; Denayer, J.; Ocakoglu, R.; Baron, G.; Muñoz, J. A.; Thybaut, J.; Marin, G. B.; *Catal. Today* **2001**, *65*, 111.
29. Deldari, H.; *Appl. Catal. A* **2005**, *293*,1.
30. Rezgui, Y.; Guemini, M.; *Appl. Catal. A* **2005**, *282*, 45.
31. Martens, J. A. ; Jacobs, P. A. ; Weitkamp, J.; *Appl. Catal.* **1986**, *100*, 541.